

**Mechanical stability of lipid membranes decorated with Dextran Sulfate**

Candelaria I. Cámara<sup>1,2</sup>, Florencia E. Lurgo<sup>1,2</sup>, Maria Laura Fanani<sup>1,2</sup>, Natalia Wilke<sup>1,2\*</sup>

<sup>1</sup> Universidad Nacional de Córdoba. Facultad de Ciencias Químicas. Departamento de Química Biológica Ranwel Caputto. Ciudad Universitaria, X5000HUA, Córdoba, Argentina

<sup>2</sup> CONICET. Universidad Nacional de Córdoba. Centro de Investigaciones en Química Biológica de Córdoba (CIQUIBIC), Ciudad Universitaria, X5000HUA, Córdoba, Argentina.

\* To whom correspondence should be addressed:

E-mail: wilke@mail.fcq.unc.edu.ar

Phone: +54-351-5353855.

**Index**

**SM1- Compression isotherms**

**SM2- BAM images**

**SM3- Size distribution of LUVs determined by DLS.**

**SM4- Rupture and permeability of LUVs upon detergent.**

**SM5- Determination of shear viscosity of the used solutions.**

**SM6- Determination of shape fluctuation of GUVs**

SM1- Compression isotherms

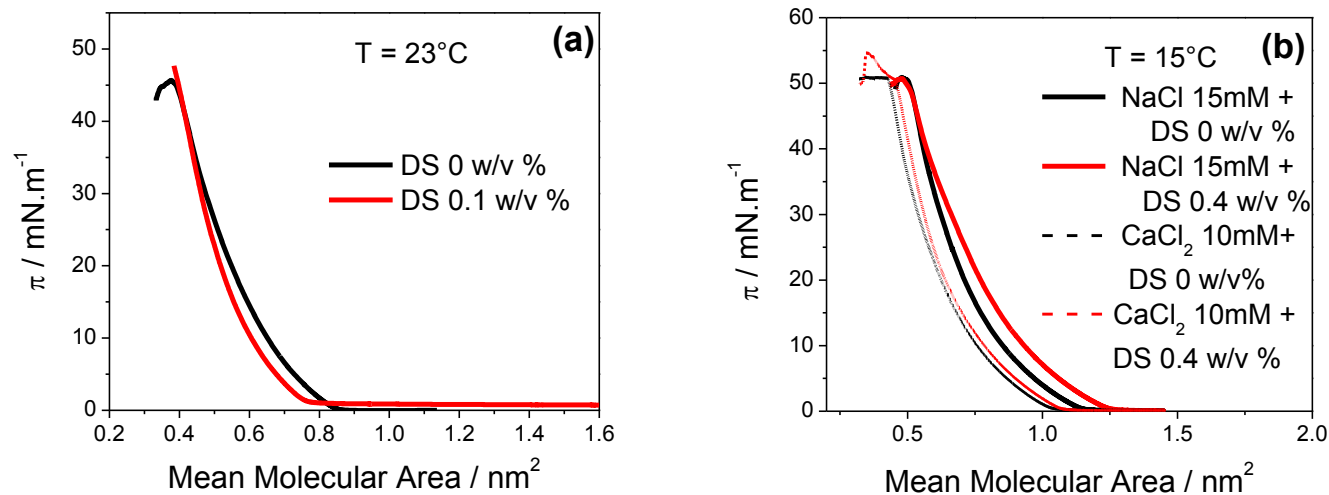


**Figure S1:** Surface pressure - average molecular area compression isotherms for **(a)** DOTAP: DOPC 1:9 and **(b)** DOPG: DPPC 1:1; in the absence and in the presence of **(a)** 0.1 w/v % and **(b)** 0.4 w/v % of DS. Experimental conditions: **(a)** 145 mM NaCl and **(b)** 15 mM NaCl or 10mM CaCl<sub>2</sub>. The surface-pressure vs mean molecular areas were similar (within errors) in the absence and in the presence of DS (typical errors: 0.03  $\text{nm}^2$  at low and 0.01  $\text{nm}^2$  at high surface pressures).

**SM2- BAM images**

**Table S1:** Surface pressure at which domains appear in the BAM images.

<b>Surface pressure of appearance of domains (mN/m)</b>				
<b>Condition</b>	<b>DOPG/DPPC 1:1 T = 15°C</b>	<b>DPPC T = 24°C</b>	<b>Condition</b>	<b>DOPG/DPPC 1:1 T = 15°C</b>
<b>NaCl 145mM</b>	24 ± 2	8±1	<b>NaCl 15mM</b>	24±1
<b>NaCl 145mM + DS 0.1 w/v %</b>	19 ± 2	8±1	<b>NaCl 15mM + DS 0.4 w/v %</b>	15±1
<b>NaCl 145mM + CaCl<sub>2</sub> 10 mM</b>	17 ± 2	6±1	<b>CaCl<sub>2</sub> 10 mM</b>	15.1±1
<b>NaCl 145mM + CaCl<sub>2</sub> 10 mM + DS 0.1 w/v %</b>	12 ± 2	4±1	<b>CaCl<sub>2</sub> 10 mM + DS 0.4 w/v %</b>	5.5±0.5

DOTAP/DOPC 1:9

NaCl 145 mM

NaCl 145 mM, DS 0.1 w/v %

30 mN.m<sup>-1</sup>

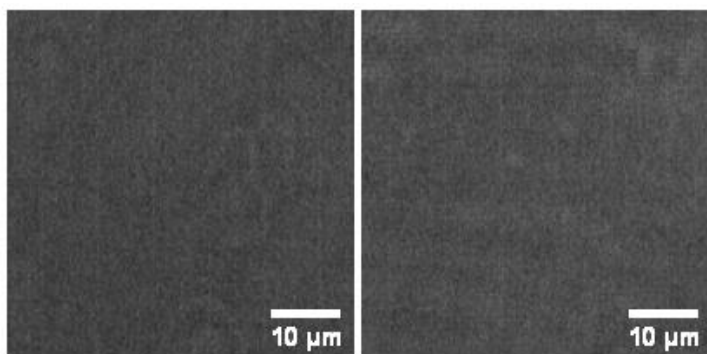


**Figure S2:** Representative BAM images of monolayers composed of DOTAP:DOPC 1:9, in the absence and in the presence of 0.1% w/v of DS at the indicated surface pressures. The gray levels were rescaled from the original 0–255 range to 0–73 for better visualization. Despite images look similar, the determined gray level values were  $20.2 \pm 0.5$  (without DS) and  $23.6 \pm 0.2$  (with DS).

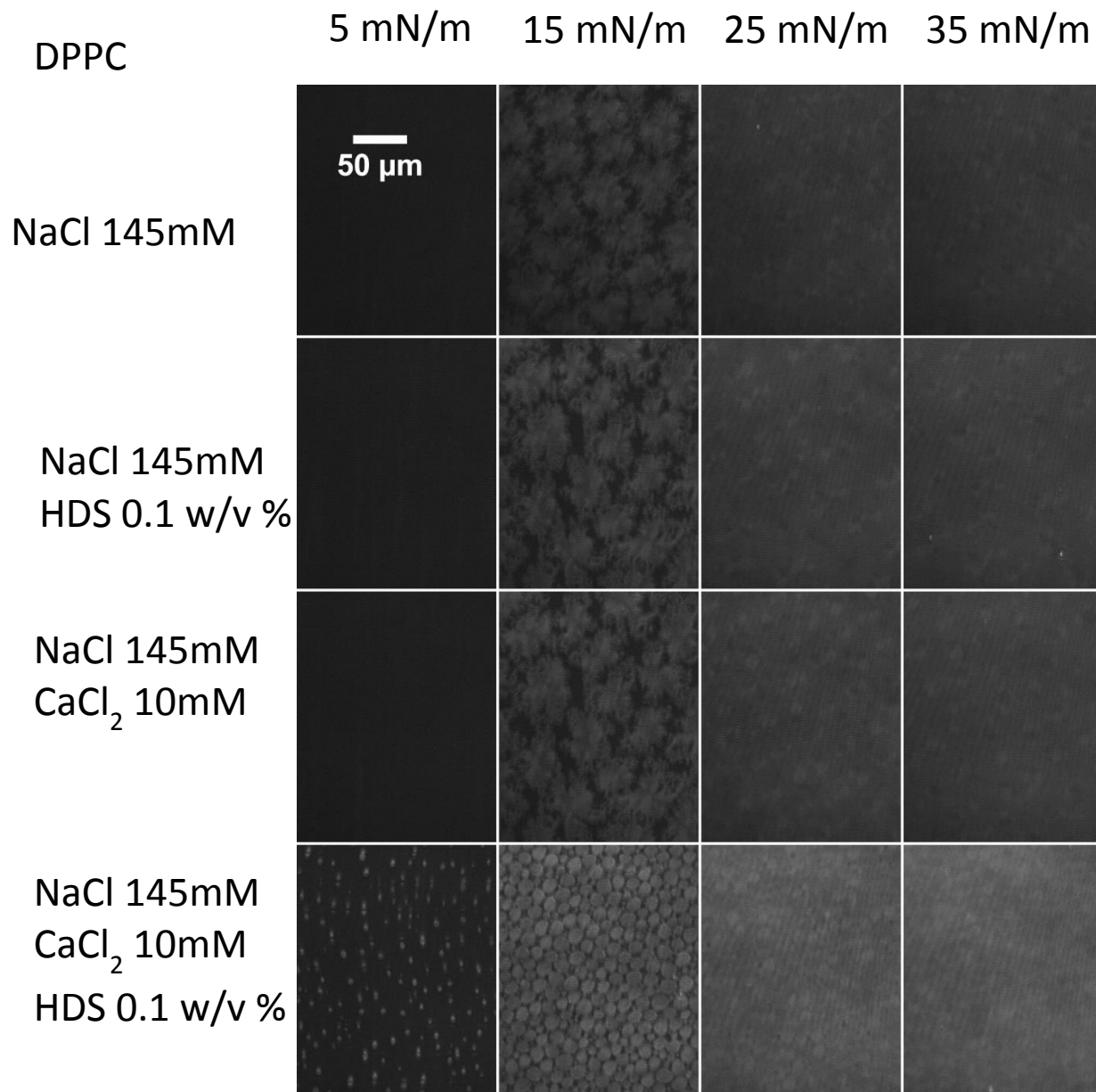


**Figure S3:** Representative BAM images of monolayers composed of DPPC in the absence and in the presence of 0.1 w/v % of DS at the indicated surface pressures. The gray levels were rescaled from the original 0–255 range to 9–52 for better visualization. The brighter regions correspond to the condensed phase.

~ S6 ~

5 mN/m    15 mN/m    25 mN/m    35 mN/m

DOPG/DPPC 1:1

NaCl 145mM

NaCl 145mM

HDS 0.1 w/v %

NaCl 145mM

CaCl<sub>2</sub> 10mM

NaCl 145mM

CaCl<sub>2</sub> 10mM

HDS 0.1 w/v %

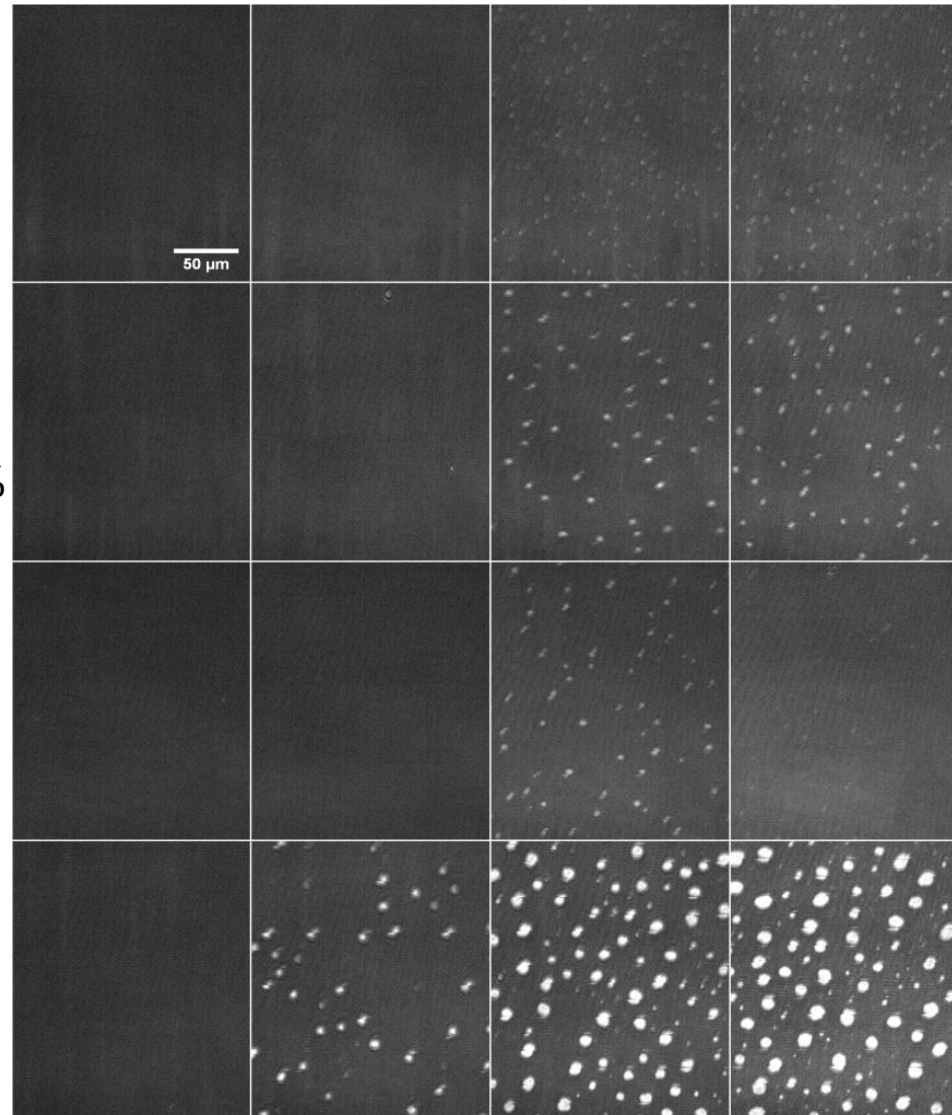


**Figure S4:** Representative BAM images of monolayers composed of DOPG:DPPC 1:1 in the absence and in the presence of 0.1 w/v % of DS at the indicated surface pressures. The gray levels were rescaled from the original 0–255 range to 9–52 for better visualization. The brighter regions correspond to the condensed phase.

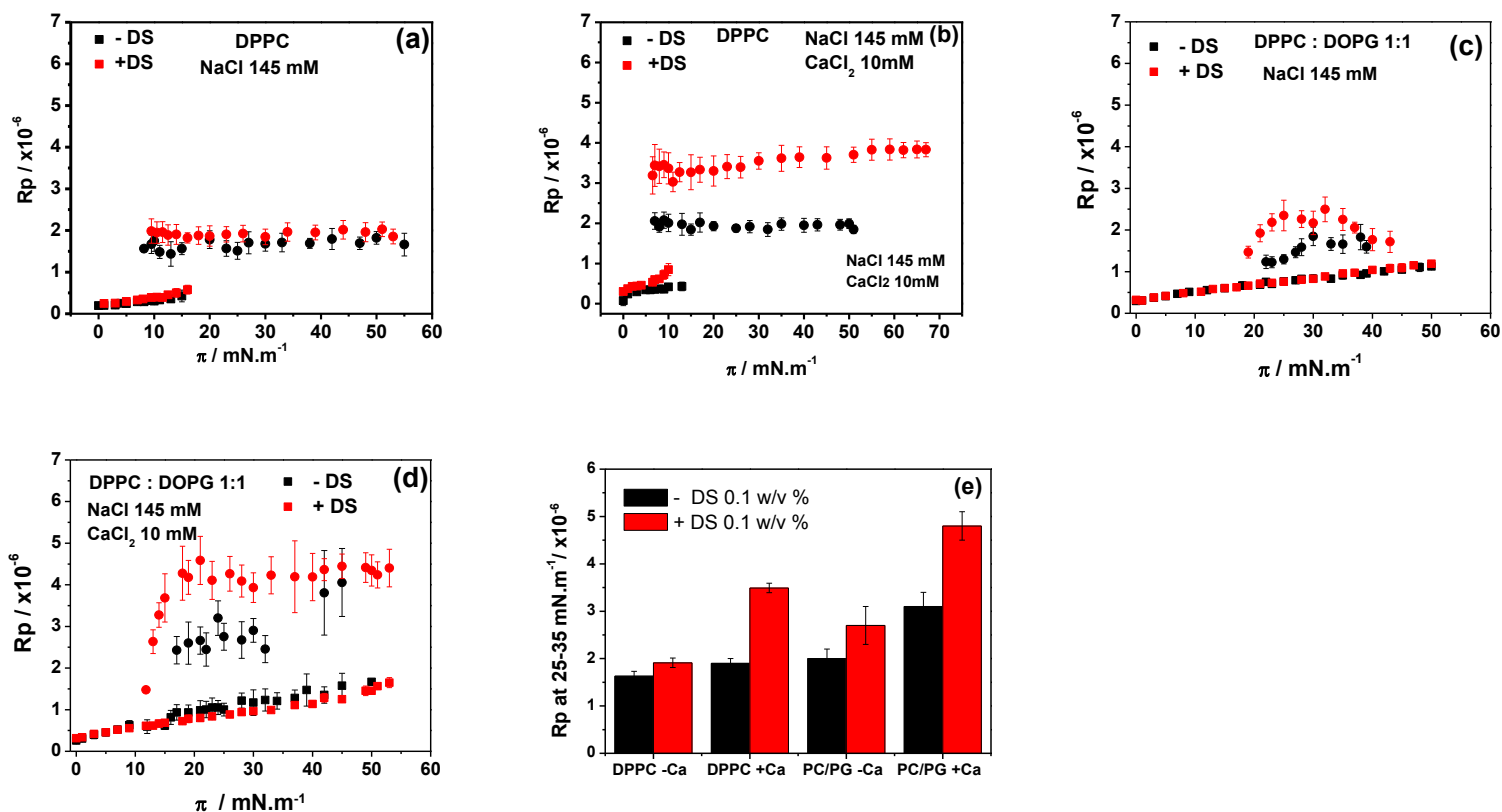


**Figure S5:** Average reflected light intensity of BAM images as those shown in figure S3 and S4 as a function of surface pressure for (a-b) DPPC and (c-d) DOPG:DPPC 1:1 monolayer in the absence (**black**) and in the presence of 0.1 w/v % DS (**red**). Subphase composition: **(a)** 145 mM NaCl, **(b)** 145 mM NaCl + 10 mM CaCl<sub>2</sub>. The  $R_p$  values correspond to regions of the monolayer in the expanded phase ( $\blacksquare$ ) or in the condensed phase ( $\bullet$ ). Each data correspond to average  $\pm$  SD of 6 different regions in at least 4 images. **(e)** Mean value of  $R_p$  in the range of 25-35 mN.m<sup>-1</sup> for each monolayer condition in the absence (**black**) and in the presence (**red**) of 0.1 % w/v DS. The mean values of  $R_p$  were taken from the condensed phase.

SM3- Size distribution of LUVs determined by DLS.

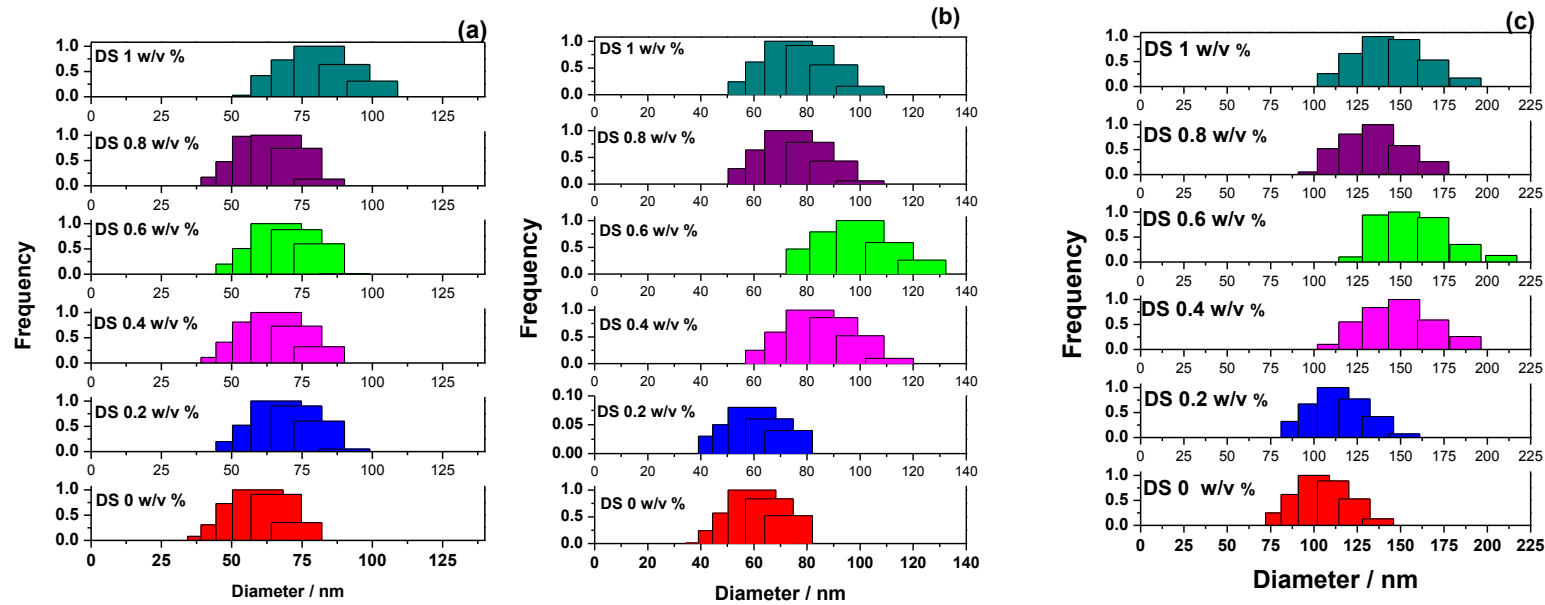


**Figure S6:** LUV's size distribution (Frequency (intensity) vs Diameter) for: DOPG/DPPC 1:1 in NaCl 15mM **(a)** or CaCl<sub>2</sub> 10mM **(b)**; DOTAP: DOPC 1:9 in NaCl 145 mM **(c)**. Increasing DS concentration from the bottom (0 w/v %) to the top (1 w/v %).



**SM4- Rupture and permeability of LUVs upon detergent addition.**

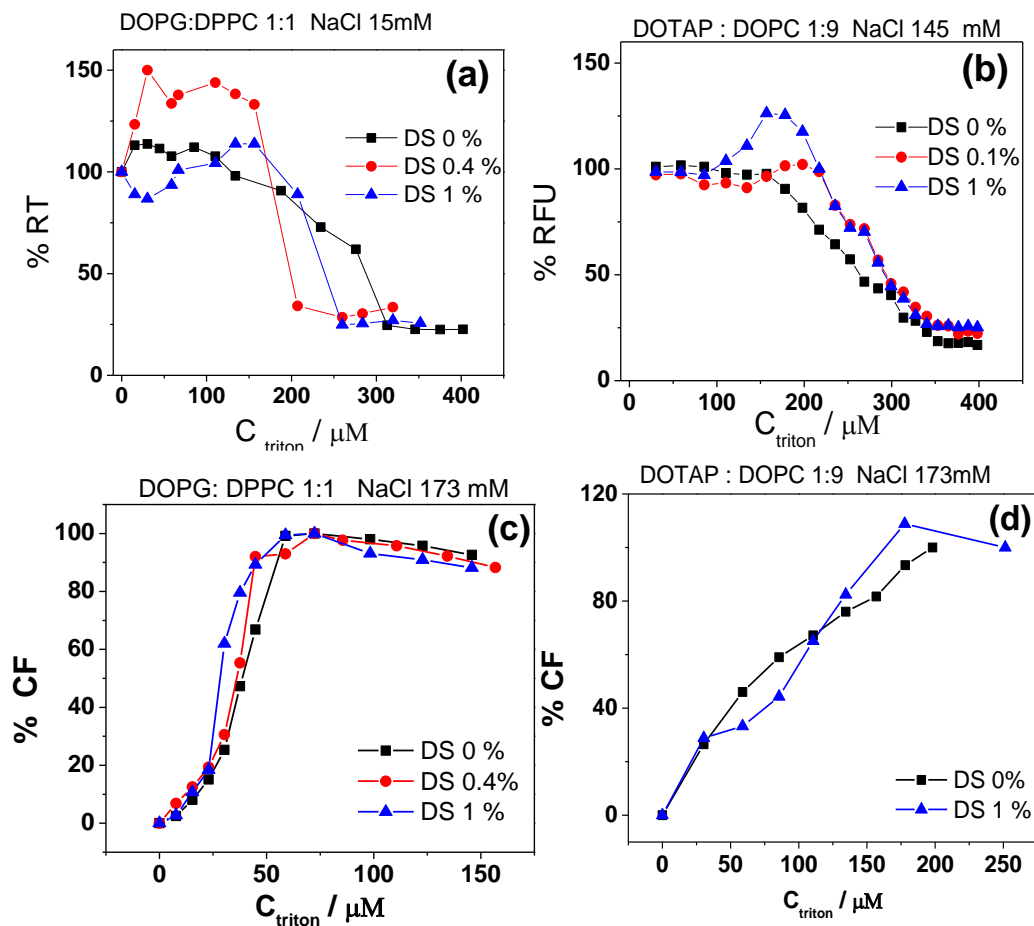


**Figure S7:** (a-b) Percent of relative turbidity (%RT) and (c-d) Percent of released carboxyfluorescein (% CF) vs triton concentration for LUVs composed of DOPG: DPPC 1:1 (a-c) and DOTAP:DOPC 1:9 (b-d). Subphase composition: 0, 0.4 and 1 w/v % of DS in NaCl 15 mM (a), 145 mM (b) and 173 mM (c-d).

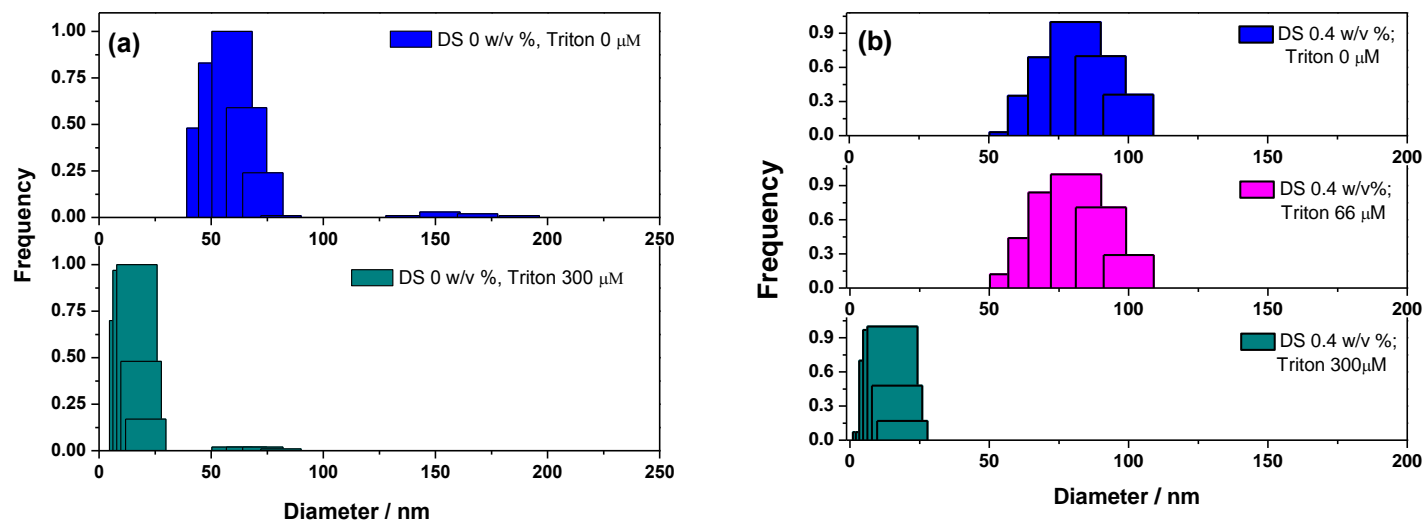


**Figure S8:** LUV's size distribution (Frequency (intensity) vs Diameter) for DOPG/DPPC 1:1 in absence **(a)** and presence of DS 0.4 w/v % **(b)** in NaCl 15mM; at 0  $\mu\text{M}$ , 66  $\mu\text{M}$  and 300  $\mu\text{M}$  Triton concentration.

**SM5- Determination of the shear viscosity of the used solutions.**

The rheological characterization of the solutions was carried out using a rotational Anton Paar Physica MCR 301 controlled strain rheometer. A 50 mm cone-plate (CP50) geometry with an angle of  $\alpha=1.006^\circ$  was used and the volumes employed were 0.7 mL. Shear stress ( $\tau$  / Pa) as a function of shear rate ( $\dot{\gamma}$  / Hz) was measured in a range of shear rate between 10-10000 Hz.

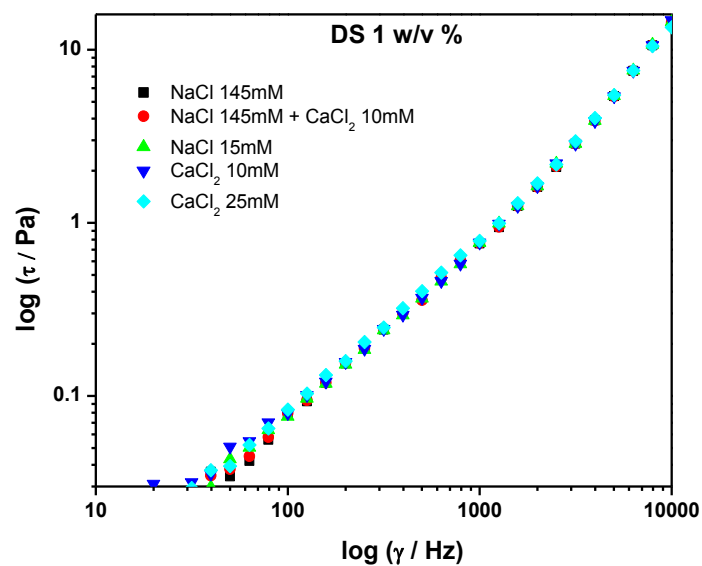


**Figure S9:** Double logarithm plot of shear stress vs shear rate for solutions containing DS 1 w/v % and NaCl 145 mM; NaCl 145 mM + CaCl<sub>2</sub> 10mM; NaCl 15 mM; CaCl<sub>2</sub> 10mM and CaCl<sub>2</sub> 25mM. T = 20°C

**Table S2:** Shear Viscosity values for DS 1 w/v % and the indicated salts at 20°C and 100 Hz. Shear viscosity was calculated as  $\tau$  (shear stress/Pa)/ $\dot{\gamma}$  (shear rate / Hz). The data shown are the average values ( $\pm$  standard deviation) of two independent experiments.

<b>Condition</b>	<b>Shear Viscosity /Pa . s</b>
<b>NaCl 145mM without DS*</b>	$(7.7 \pm 0.1) \times 10^{-4}$
<b>NaCl 145 mM + DS 1% w/v</b>	$(7.7 \pm 0.2) \times 10^{-4}$
<b>NaCl 145mM + CaCl<sub>2</sub> 10mM + DS 1% w/v</b>	$(7.89 \pm 0.08) \times 10^{-4}$
<b>NaCl 15Mm + DS 1% w/v</b>	$(7.4 \pm 0.2) \times 10^{-4}$
<b>CaCl<sub>2</sub> 10mM + DS 1% w/v</b>	$(7.6 \pm 0.9) \times 10^{-4}$
<b>CaCl<sub>2</sub> 25mM + DS 1% w/v</b>	$(7.80 \pm 0.08) \times 10^{-4}$

\* Control viscosity value for NaCl 145mM without DS.

SM6- Determination of the shape fluctuation of GUVs: Statistical analysis of GUV's shape

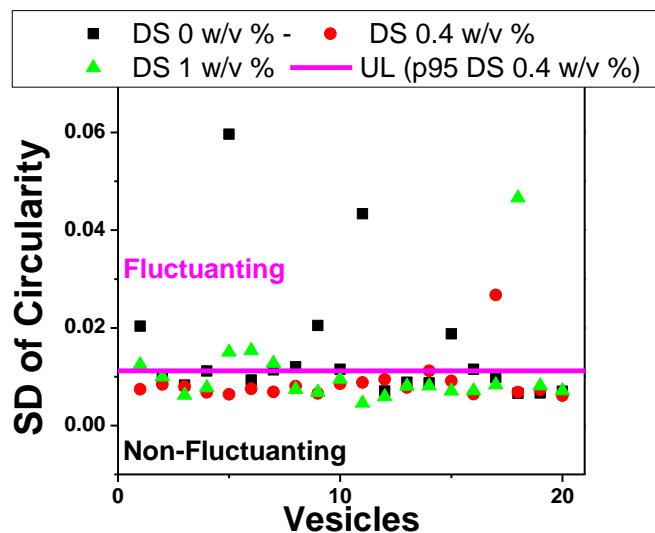


**Figure S10:** Standard deviation of the circularity for each individual GUV. Analyzed treatments: DS 0, 0.4 and 1 w/v % for DOPG : DPPC 1: 1 in CaCl<sub>2</sub> 10mM. The **magenta line** represent the upper limit used to define a GUV as “fluctuating” or “non-fluctuating”, i.e. the value of P95<sup>th</sup> for the data of the Standard deviation of the circularity of the less fluctuating population, which in this case corresponds to the treatment with DS 0.4 w/v % (see table S4).

**Table S3:** Average Circularity ( $\bar{C}$ ) with the corresponding standard deviation ( $SD\bar{C}$ ) for one of the experiment performed with DOPG:DPPC 1:1 in  $CaCl_2$  10 mM and with different DS concentration.

GUV number	DS concentration / % w/v					
	0 w/v %		0.4 w/v %		1.0 w/v %	
	$\bar{C}^{DS\ 0\%}$	$SD\bar{C}^{DS\ 0\%}$	$\bar{C}^{DS\ 0.4\%}$	$SD\bar{C}^{DS\ 0.4\%}$	$\bar{C}^{DS\ 1\%}$	$SD\bar{C}^{DS\ 1\%}$
1	0.89886	0.02036	0.8956	0.00744	0.87818	0.01242
2	0.90164	0.00963	0.90918	0.00841	0.91804	0.00993
3	0.90738	0.00829	0.90681	0.00795	0.90957	0.00619
4	0.89023	0.01116	0.91058	0.00681	0.89882	0.00772
5	0.71645	0.05963	0.91091	0.0064	0.89624	0.01503
6	0.9161	0.00932	0.91137	0.00752	0.9147	0.01533
7	0.88967	0.0114	0.90844	0.00688	0.89999	0.01272
8	0.88989	0.01202	0.91324	0.00807	0.90411	0.00739
9	0.90245	0.02049	0.9181	0.00658	0.89879	0.00679
10	0.87234	0.0115	0.91995	0.00857	0.89635	0.00952
11	0.64584	0.04333	0.90733	0.00883	0.90306	0.00461
12	0.89313	0.00708	0.91666	0.00943	0.89927	0.0059
13	0.90675	0.00884	0.91355	0.0078	0.8948	0.00806
14	0.90179	0.00872	0.90684	0.01121	0.90005	0.00812
15	0.87218	0.01875	0.91202	0.00914	0.90475	0.00706
16	0.90895	0.01151	0.90837	0.00642	0.90146	0.00712
17	0.90013	0.00979	0.80833	0.02674	0.90257	0.00833
18	0.89636	0.00663	0.9036	0.00685	0.75533	0.04659
19	0.90407	0.00665	0.90488	0.00732	0.91725	0.00813
20	0.90062	0.007	0.90367	0.00612	0.89698	0.0071

**Table S4:** Values of P95<sup>th</sup> for  $SD\bar{C}$  at different DS concentration for the experiments of table S1. Highlighted are the lower values of P95<sup>th</sup>, corresponding to a DS concentration of 0.4% w/v. This value was taken as the upper limit, and correspond to the magenta lines shown in figure SM6-1.

DS (w/v %)	P95 <sup>th</sup> $SD\bar{C}$
0	0.0433
0.4	0.0112
1	0.0153